Electromagnetic signals from bare strange stars

Massimo Mannarelli* and Giulia Pagliaroli†
INFN, Laboratori Nazionali del Gran Sasso, Via G. Acitelli, 22, I-67100 Assergi (AQ), Italy

Alessandro Parisi‡ and Luigi Pilo§
Dipartimento di Scienze Fisiche e Chimiche, Università di L'Aquila, I-67010 L'Aquila, Italy
INFN, Laboratori Nazionali del Gran Sasso, Via G. Acitelli, 22, I-67100 Assergi (AQ), Italy

arXiv:1403.0128v2 [hep-ph] 21 May 2014

The crystalline color superconducting phase is believed to be the ground state of deconfined quark matter for sufficiently large values of the strange quark mass. This phase has the remarkable property of being more rigid than any known material. It can therefore sustain large shear stresses, supporting torsional oscillations of large amplitude. The torsional oscillations could lead to observable electromagnetic signals if strange stars have a crystalline color superconducting crust. Indeed, considering a simple model of strange star with a bare quark matter surface, it turns out that a positive charge is localized in a narrow shell about ten Fermi thick beneath the star surface. The electrons needed to neutralize the positive charge of quarks spill in the star exterior forming an electromagnetically bounded atmosphere hundreds of Fermi thick. When a torsional oscillation is excited, for example by a stellar glitch, the positive charge oscillates with typical kHz frequencies, for a crust thickness of about one-tenth of the stellar radius, to hundreds of Hz, for a crust thickness of about nine-tenths of the stellar radius. Higher frequencies, of the order of few GHz, can be reached if the star crust is of the order of few centimeters thick. We estimate the emitted power considering emission by an oscillating magnetic dipole, finding that it can be quite large, of the order of 10^{45} erg/s for a thin crust. The associated relaxation times are very uncertain, with values ranging between microseconds and minutes, depending on the crust thickness. The radiated photons will be in part absorbed by the electronic atmosphere, but a sizable fraction of them should be emitted by the star.

I. INTRODUCTION

One of the routes for studying the properties of matter at very high densities is by the inspection of the properties of compact stellar objects (CSOs). These are stars having a mass of $1 - 2M_\odot$ and a radius of about 10 km, typically observed as pulsars. Baryonic matter inside a CSO is squeezed at densities about a factor 3-5 larger than in heavy nuclei. From a simple geometrical reasoning one can argue that in these conditions baryons are likely to lose their identity [1] and a new form of matter should be realized.

One possibility is that the extremely high densities and low temperatures may favor the transition from nuclear matter to deconfined quark matter in the core of the CSO [2–5]. In this case compact (hybrid) stars featuring quark cores and a crust of standard nuclear matter would exist.

A second possibility is that strange matter is the ground state of the hadrons [6]. In this case at high densities there should exist the possibility of converting nuclear matter to deconfined matter. The resulting CSO would be a strange star [7, 8], *i.e* a CSO completely constituted of deconfined matter, see [9] for a review.

Unfortunately these two possibilities cannot be checked by first principle calculations. Indeed at the densities relevant for CSOs, quantum chromodynamics (QCD) is nonperturbative, because the typical energy scale is about $\Lambda_{\rm QCD}$. Moreover, lattice QCD simulations at large baryonic densities are unfeasible because of the so-called sign problem [10], see [11] for a recent review and [12] for a study of an inhomogeneous phase.

Although not firmly established by first principles, it is reasonable to expect that if deconfined quark matter is present, it should be in a color superconducting (CSC) phase [13–15]. The reason is that the critical temperature of color superconductors is large, $T_c \simeq 0.57\Delta$, where $\Delta \sim 5 - 100$ MeV is the gap parameter. For the greatest part of the CSO lifetime, the temperature is much lower than this critical temperature and the CSC phase is thermodynamically favored.

It is widely accepted that at asymptotic densities, when the up, down and strange quarks can be treated as massless, the color-flavor locked (CFL) phase [16] is the ground state of matter. This phase is energetically favored because quarks of all flavors and of all colors form standard Cooper pairs, thus maximizing the free energy gain. However, considering realistic conditions realizable within CSOs a different CSC phase could be realized. The reason is that the nonzero and possibly large value of the strange quark mass, M_s, combined with the requirement of beta equilibrium, electromagnetic and color neutrality, tends to pull apart the Fermi spheres of quarks with different flavors [17]. The mismatch between the

*Electronic address: massimo@lngs.infn.it
†Electronic address: giulia.pagliaroli@lngs.infn.it
‡Electronic address: alessandro.parisi@lngs.infn.it
§Electronic address: luigi.pilo@aquila.infn.it

Fermi spheres is proportional to M_s^2/μ, where

$$\mu = \frac{\mu_u + \mu_d + \mu_s}{3}\,, \tag{1}$$

is the average quark chemical potential. The free energy price of having simultaneous pairing of three-flavor quark matter increases with increasing values of M_s^2/μ. Since the free energy gain is proportional to the CFL gap parameter, $\Delta_{\rm CFL}$, if $M_s^2/\mu > c\Delta_{\rm CFL}$, with c a number of order 1 [18], a different and less symmetric CSC phase should be favored. One possibility is that the crystalline color superconducting (CCSC) phase is realized [15, 19–21]. In this phase quarks form Cooper pairs with nonzero total momentum, and there is no free energy cost proportional to M_s^2/μ. The only free energy cost is due to the formation of counterpropagating currents; see for example the qualitative discussion in [21].

Actually, with increasing values of M_s^2/μ various inhomogeneous CSC phases can be realized, because the system has many degrees of freedom [15]. The CCSC phase should be favored for certain values of the chemical potential mismatch. In reality, the CCSC phase is not one single phase but a collection of phases, characterized by their crystalline arrangements, which are favored for different values of M_s^2/μ. The Ginzburg-Landau (GL) analysis of [20] has shown that in three-flavor quark matter there are two good candidate structures that are energetically favored for

$$2.9\Delta_{\rm CFL} \lesssim \frac{M_s^2}{\mu} \lesssim 10.4\Delta_{\rm CFL}\,. \tag{2}$$

This range of values is certainly model dependent, moreover the GL expansion is under poor quantitative control [15]. For this reason we shall consider strange star models in which both the CFL phase and the CCSC phase are realized. Since the CFL phase is expected to be favored at high densities, we shall assume that it is realized in the core of the CSO. The CCSC phase is favored at smaller densities and constitutes the crust of the CSO. The radius, R_c, at which the CFL core turns into the CCSC crust will be used as a free parameter. We shall restrict our analysis to bare strange stars [7], meaning that we shall assume that on the top of the strange star surface there is no other layer of baryonic matter.

Our model of strange star resembles the typical onion structure of a standard neutron star with a solid crust and a superfluid core. It is similar to the model discussed in [22] for studying $r-$mode oscillations. In that work the core radius was determined using a microscopic approach; instead we treat R_c as a free parameter.

One quantitative difference between our model and standard neutron star models, is that the CCSC phase is extremely rigid, much more rigid than the ironlike crust. The shear modulus of the energetically favored phase can be obtained studying the low energy oscillations of the condensate modulation [23–26]. In particular, the low energy expansion of the GL Lagrangian of [26] leads to a shear modulus

$$\nu \simeq \nu_0 \left(\frac{\Delta}{10\ {\rm MeV}}\right)^2 \left(\frac{\mu}{400\ {\rm MeV}}\right)^2\,, \tag{3}$$

where

$$\nu_0 = 2.47 \frac{\rm MeV}{\rm fm^3}\,, \tag{4}$$

will be our reference value. The reader is warned that the actual value of the shear modulus might differ from ν_0 by a large amount because of the various approximations used in [26]. The value of Δ is also uncertain, with reasonable values ranging between 5 MeV and 25 MeV, see the discussions in [15, 26]. Regarding the quark chemical potential, we shall consider the values obtained in the construction of hydrodynamically stable strange stars. The shear modulus of different crystalline structures is proportional to ν, with corrections of the order unity. Since in our treatment we shall only exploit the rigidness of the CCSC phase giving the order of magnitude estimates for the various computed quantities, the actual crystalline pattern is irrelevant for our purposes.

Taking into account the uncertainty in the gap parameter and in the quark chemical potential, it can be estimated that the value of ν is larger than in conventional neutron star crust (see for example [27]), by at least a factor of $20-1000$ [26]. This large value of the shear modulus is due to the fact that the typical energy density associated with the oscillations of the condensate modulation is $\mu^2\Delta^2$, where Δ is determined by the strong interaction in the antitriplet channel. Instead, in conventional neutron star the associated energy is at the electromagnetic scale.

Given the large shear modulus, one immediate consequence is that CCSC matter can sustain large deformations. In Refs. [22, 28–31] it has been studied the emission of gravitational waves by various mechanisms that induce a quadrupole deformation of the CCSC structure. See also [32] for a discussion of a different mechanism of gravitational wave emission from strange stars.

In the present paper we shall instead consider the electromagnetic (EM) emission by strange stars with a CCSC crust. Since the strange star surface confines baryonic matter but allows the leakage of electrons, it follows that at the star surface there is a charge separation at the hundreds of Fermi scale [7]. Because of the large shear modulus, our model of bare strange star can sustain large and fast torsional oscillations, leading to a periodic displacement of the surface charge. We shall see that the frequencies of torsional oscillations are of the order of MHz if the crust is hundreds of meters thick. Lower frequencies are reached if the crust is a few kilometers thick; GHz frequencies are reached if the crust is few centimeters thick.

The amplitude of the oscillations at the star surface is in any case of the order of centimeters, leading to an enormous emitted radiation, of the order of 10^{41} erg/s, steeply increasing for thin crusts. Thus the oscillation

energy should be radiated away very efficiently, on time scales of milliseconds or even microseconds for a thin crust and of the order of hundreds of seconds for a thick crust. More in detail, we shall determine the frequency, the amplitude, the damping times and the emitted power as a function of the various parameters that characterize the strange star.

This paper is organized as follows. In Sec. II we discuss spherically symmetric strange stars in hydrodynamical equilibrium. In Sec. III we determine the charge distribution close to the surface of the strange star. In Sec. IV we study the torsional oscillations of the strange star, estimating the frequencies, the emitted power and the decay time as a function of the various parameters of the model. We draw our conclusions and a possible connection with astronomical observations in Sec. V.

II. EQUILIBRIUM CONFIGURATIONS OF SPHERICALLY SYMMETRIC STRANGE STARS

For a spherically symmetric nonrotating star, the unperturbed background can be described by the static metric

$$ds^2 = g_{\mu\nu}dx^\mu dx^\nu = -e^{2\Phi(r)}dt^2 + e^{2\Lambda(r)}dr^2 + r^2 d\Omega^2 \,. \quad (5)$$

The relation between the function $\Lambda(r)$ and the mass distribution $m(r)$ is given by the solution of Einstein's equations inside the star, namely

$$e^{2\Lambda(r)} = \left[1 - \frac{2m(r)G}{r}\right]^{-1} , \; m(r) = \int_0^r dr'\, r'^2\, \rho(r') \,, \quad (6)$$

where $\rho(r)$ is the energy density of the fluid. The equilibrium structure is obtained by solving the Tolman-Oppenheimer-Volkov (TOV) equation

$$\frac{\partial p}{\partial r} = -\frac{G(p+\rho)\left(m + 4\pi p\, r^3\right)}{r(r - 2G\, m)} \,, \quad (7)$$

once the equation of state (EoS) $p(\rho)$ is specified. The star radius, R, is determined by the boundary condition on the pressure $p(R) = 0$, simply meaning that the pressure at the surface of the star should vanish.

The gravitational potential Φ can be found from

$$\frac{\partial \Phi}{\partial r} = \frac{G\left(m + 4\pi\, p\, r^3\right)}{r(r - 2Gm)} \,, \quad (8)$$

once p is derived from the solution of Eq. (7). Outside the star, for $r > R$, defining $m(R) = M$, we have that

$$e^{2\Lambda(r)} = \left(1 - \frac{2MG}{r}\right)^{-1} , \qquad e^{2\Phi(r)} = 1 - \frac{2MG}{r} \,. \quad (9)$$

In the present work we consider a simple strange star model, entirely composed of deconfined three-flavor quark matter in the CSC phase. The detailed form of the CSC phase is not important here, because quark pairing should account for a small variation of the quark matter EoS.

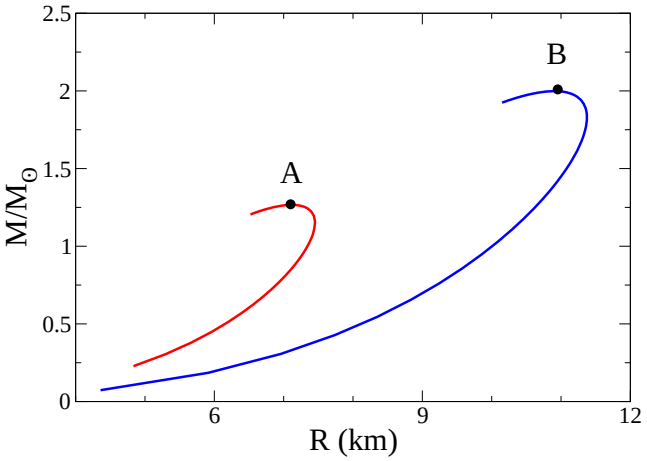

FIG. 1: Mass radius relation for strange stars with the EoS given in Eq. (10) for the two sets of parameters values discussed in the text. Changing these parameters it is possible to span a large range of values of mass and radius. The black dots represent the equilibrium structure assumed as reference models in this paper.

Since for the range of densities attainable in compact stars QCD perturbative calculations are not trustable, we use the general parameterization of the EoS given in [33]

$$\Omega_{\rm QM} = -\frac{3}{4\pi^2}a_4\mu^4 + \frac{3}{4\pi^2}a_2\mu^2 + B_{\rm eff} \,, \quad (10)$$

where a_4, a_2 and $B_{\rm eff}$ are independent of the average quark chemical potential μ. This parameterization can be seen as a Taylor expansion of the grand potential, with phenomenological coefficients (see [33] for a discussion of the relevant range of values of each parameter). In order to take into account the impact of the uncertainty of these coefficients on our results, we consider two extreme situations, namely A ($a_4 = 0.7$, $a_2 = (200\ {\rm MeV})^2$ and $B_{\rm eff} = (165\ {\rm MeV})^4$) and B ($a_4 = 0.7$, $a_2 = 0$ and $B_{\rm eff} = (145\ {\rm MeV})^4$). In Fig. 1 we report the mass-radius sequences obtained solving the TOV equations using the above EoS for the two different sets of parameters. The largest attainable mass with each set will be our reference model, represented as a black dot in Fig. 1. In detail: - Model A, with a total mass of $M = 1.27 M_\odot$, $R \simeq 7.1$ km and $\rho_c \simeq 5 * 10^{15}{\rm g/cm}^3$; - Model B, with $M \simeq 2.0 M_\odot$, $R \simeq 10.9$ km and $\rho_c \simeq 2 * 10^{15}{\rm g/cm}^3$. The presence of electric charge is expected to produce corrections on masses and radii of strange quark stars at the 15% and 5% levels, respectively [34].

In both models we assume that at a certain radial distance, $R_c = aR$ with $0 \leq a \leq 1$, there is a phase tran-

sition between the CFL phase and the CCSC phase. In Fig. 2 we show a pictorial description of the star structure. Since the values of M_s and of the gap parameters are unknown, it is not possible to determine from first principles the radial distance at which the CFL phase turns into the CCSC phase. For this reason we treat a as a parameter. More in detail, in our model we are assuming that the CFL-CCSC phase transition does not change in an appreciable way the EoS. Thus, our assumption is that at a given R_c the pressure of the CCSC phase and of the CFL phase are equal, but the difference between the pressure of these two phases is always small in the sense that computing the star mass and radius using only a CFL EoS or only a CCSC EoS does not change the results in an appreciable way. This is a fair approximation as far as the gap parameter in both phases are similar and much less than the average chemical potential. Our model is basically the model discussed in [22], but we treat a as a free parameter, whereas they compute it by a microscopic theory.

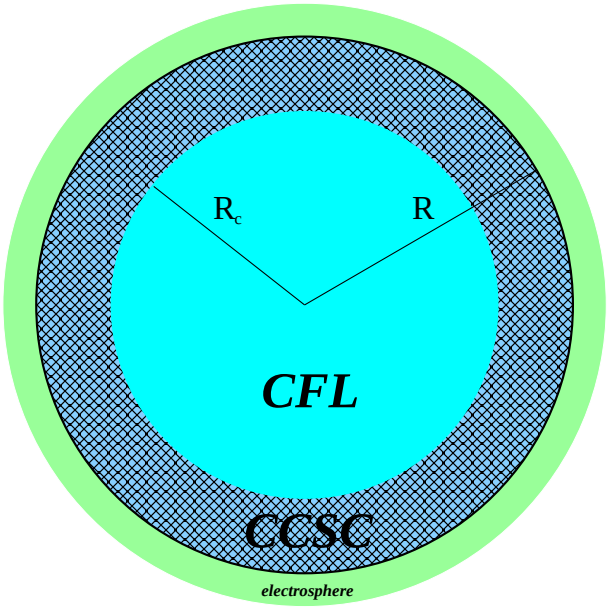

FIG. 2: Sketch of the structure of the considered bare strange star model. The star *core* extends up to a radius R_c, and is made by color-flavor locked matter. The *crust* is made by the extremely rigid crystalline color superconducting matter. The star radius, R, is determined by the solution of the TOV equation (7) with the EoS in Eq. (10). We treat the core radius, $R_c = aR$, as a free parameter. The strange star is surrounded by a cloud of electrons, the *electrosphere*, having a width (not in scale in the figure) of hundreds of Fermi, see Sec. III.

III. CHARGE DISTRIBUTION

It is very interesting to study the charge distribution close to the surface of the strange star. The reason is that quarks are confined inside the strange star by the strong interaction, while electrons can leak by a certain distance outside the star and are bound only by the electromagnetic interaction [7]. As we shall see in detail below, electrons form an *electrosphere* hundreds of Fermi thick on the top of the star surface. This negative charge is compensated by a positive charge of quarks in a narrow layer, about 10 fm thick, beneath the star surface.

Let us see how this charge separation happens. At equilibrium, the chemical potentials associated to any free particle species must be constant, *i.e.* space independent, otherwise particles would move to compensate the chemical potential difference. However, in the presence of an electrostatic potential, ϕ, the density of particles can be space dependent. In the local density approximation this fact can be taken into account defining the space dependent effective chemical potential

$$\mu_i(\boldsymbol{x}) = \mu_i + eQ_i\phi(\boldsymbol{x})\,, \tag{11}$$

where Q_i is the charge of the species i, in units of the electric charge, e. Note that because of the weak process $u + d \leftrightarrow u + s$ one has $\mu_s(\boldsymbol{x}) = \mu_d(\boldsymbol{x})$. Note also that the average chemical potential, μ, see Eq. (1), is space independent; indeed $\mu_u(\boldsymbol{x}) + \mu_d(\boldsymbol{x}) + \mu_s(\boldsymbol{x}) = \mu_u + \mu_d + \mu_s = 3\mu$.

To simplify the charge distribution treatment, we shall assume that the leading effect of color interactions is to provide confinement of quarks in the interior of the star [7]. This is a good approximation if the subleading effect of color interactions is the quark condensation. Indeed quark condensation is expected to produce corrections to our results of the order Δ/M_s. Since the surface of the star is in the CCSC phase it amounts to less than 10% corrections. We also neglect the fact that in the CCSC phase the $U(1)_{\rm em}$ is rotated to a $\tilde{U}(1)$, because the mixing angle between the photon and the pertinent color field is small [14–16].

Therefore, we approximate the number density of the fermionic species, n_i, as a free Fermi gas, meaning that

$$n_i(\boldsymbol{x}) = C_i\frac{k_{F,i}(\boldsymbol{x})^3}{3\pi^2}\,, \tag{12}$$

where C_i is a factor taking into account the color degrees of freedom and $k_{F,i}(\boldsymbol{x}) = \sqrt{\mu_i(\boldsymbol{x})^2 - m_i^2}$ is the Fermi momentum, with m_i the mass.

The number density of quarks ends abruptly at the surface of the star, but the number density of electrons extends over distances $r > R$, determining the thickness of the electrosphere. If the charge distribution varies in a region much smaller than the star radius, it is possible to approximate the geometry of the interface as planar. We shall assume that this is the case and then check that it is a good approximation. For a planar interface Poisson's equation reads

$$\frac{d^2\phi}{dz^2} = e\sum_i Q_i\, n_i(z)\,, \tag{13}$$

where z measures the distance from the quark matter discontinuity, located at $z = 0$; the star interior corresponding to $z < 0$.

Two boundary conditions are obtained requiring that the charge density vanishes far from the interface. For the sake of notation we define

$$V(z) = \mu_e(z) = \mu_e - e\phi(z)\,, \tag{14}$$

and we can rewrite the Poisson's equation as

$$\frac{d^2V}{dz^2} = -\frac{4\alpha_{\rm em}}{3\pi}\sum_i Q_i\, C_i\, k_{F,i}^3\,. \tag{15}$$

Considering the weak equilibrium processes, the effective quark chemical potentials can be written as

$$\mu_u(z) = \mu - \frac{2}{3}V(z)\,,\;\; \mu_d(z) = \mu_s(z) = \mu + \frac{1}{3}V(z)\,, \tag{16}$$

and the corresponding number densities can be obtained substituting these expressions in Eq. (12). In principle the average quark chemical potential depends on the radial coordinate as well. Indeed from the EoS we can determine for any value of r the function $\mu(r)$. However, the average quark chemical potential varies on the length scale of hundreds of meters at least, much larger than the length scale of the quark charge distribution, which as we shall see below is of few tens of Fermi at most. Since the $z = 0$ region corresponds to the star surface, we can take $\mu \simeq \mu_R \equiv \mu(R)$. We report in Table I the values of these quantities for the two considered models.

No net charge is present far from the boundary, therefore we require that

$$n_e(z)_{z\to+\infty} = 0\,, \tag{17}$$

and that

$$\left[\frac{2}{3}n_u(z) - \frac{1}{3}n_d(z) - \frac{1}{3}n_s(z) - n_e(z)\right]_{z\to-\infty} = 0\,. \tag{18}$$

Neglecting the electron mass the first condition leads to $V(+\infty) = 0$; neglecting also the light quark masses the second condition leads to

$$\begin{aligned} V_q^3 \;&=\; 2\left(\mu_R - \frac{2}{3}V_q\right)^3 - \left(\mu_R + \frac{1}{3}V_q\right)^3 \\ &-\; \left[\left(\mu_R + \frac{1}{3}V_q\right)^2 - M_s^2\right]^{\frac{3}{2}} \end{aligned} \tag{19}$$

that fixes a relation among M_s, μ_R and $V_q = V(-\infty)$.

Assuming that at the crust-electrosphere interface there is no surface charge, we obtain a third boundary condition requiring that the electric field is a continuous function at $z = 0$. This boundary condition can be used to obtain an expression of the effective electron chemical potential at the surface that depends on V_q and μ, approximately given by

$$V_0 = V_q - \frac{V_q^2}{2\sqrt{3}\mu} + \mathcal{O}(V_q^3/\mu^2)\,. \tag{20}$$

Note that in most of the studies it is assumed that the quark distribution is constant, leading to $V_0 = 3/4V_q$, see [7]. Here we have instead used the free Fermi gas distribution for quarks, but the quantitative result remains basically the same: the surface potential V_0 is smaller than V_q by a not great amount.

The Poisson's equation (15) can be analytically solved for positive values of z and we find

$$V(z) = \frac{V_0}{1 + \sqrt{\frac{2\alpha_{\rm em}}{3\pi}}V_0 z} \qquad \text{for } z > 0\,. \tag{21}$$

Upon substituting the expression above in Eq. (12) (taking $C_e = 1$), one readily obtains the electron distribution for positive z.

In the interior of the star the Poisson's equation must be solved numerically. For negative values of z we obtain by a fit of the total charge distribution,

$$\sum_i Q_i\, n_i(z) = b\, e^{z/d} \qquad z \le 0\,, \tag{22}$$

where the b and d are two parameters describing the maximum charge density and the Debye screening length of the total charge distribution, respectively. The screening length has been computed in a different way in [35], finding results analogous to ours. The values of V_0 and of the fitting parameters b and d for the considered models and for two values of M_s are reported in Table I. In the interior of the star, the positive charge distribution corresponds to a shell of thickness less than 10 fm peaked at $r = R$. This result is basically independent of the considered star model and of the strange quark mass. It relies on the fact that we are considering that the dominant charge carriers in the interior of the star are gapless quarks. Indeed, in the relevant CCSC phases quarks have a linear direction dependent dispersion law, see [15, 20]. Moreover, unpaired quarks are as present as well. For this reason the Debye screening length is approximately given by the free Fermi gas expression for three massless flavors,

$$d \simeq d_{\text{Fermi gas}} = \sqrt{\frac{\pi}{8\alpha_{\rm em}\mu^2}} \sim 5\,\text{fm} \tag{23}$$

for $\mu = 300$ MeV.

The number density at the surface is approximately independent of the considered model, but depends on the chosen value of the strange quark mass. The reason is that with decreasing strange quark mass the electronic density decreases. This effect can also be seen from the values of the positive surface charge density beneath the star surface

$$Q_+ = e\sum_i Q_i \int_0^R dr\, n_i(r)\,, \tag{24}$$

reported in the last column of Table I. This positive charge is balanced by the electron negative charge outside the star. The electron distribution extends outside the star for a distance approximately given by

$(\sqrt{\frac{4\alpha_{\rm em}}{3\pi}}M_s^2/\mu)^{-1}$, see Eqs. (19), (20) and (21), of the order of hundreds of Fermi. Therefore, the length scales of both charge distributions are much less than the star radius.

Model	μ_R [MeV]	ρ_R [g/cm^3]	M_s [MeV]	d [fm]	b [MeV^3]	V_0 [MeV]	Q_+ [MeV^3 fm]
A	387	9.0×10^{14}	150	3.8	4.5×10^3	14.2	1.7×10^4
A	387	9.0×10^{14}	250	3.9	3.0×10^4	37.4	1.2×10^5
B	302	4.1×10^{14}	150	4.9	5.5×10^3	17.8	2.7×10^4
B	302	4.1×10^{14}	250	3.3	5.2×10^4	46.9	1.7×10^5

TABLE I: Values of the parameters characterizing the surface of the two considered star models. The second and third columns represent the average quark chemical potential and the matter density at the surface of the star, respectively. Considering two different values of the strange quark mass we report for each stellar model the parameters d, b and V_0 characterizing the charge distributions, see Eqs. (21) and (22), and the positive surface charge density, Q_+, see Eq. (24).

Note that, in principle, a charge separation should occur as well at R_c, at the CFL-CCSC interface; the reason being that the bulk CFL matter has vanishing electron chemical potential [14–16]. However, whatever phenomenon takes place at the CFL-CCSC interface should be screened by the overlying CCSC layer.

IV. NONRADIAL OSCILLATIONS

We now consider the possible oscillations of the above determined charge distribution. In particular, we are interested in nonradial oscillations, which can generate an EM current at the star surface.

Stars have a large number of nonradial oscillations, which can be classified as spheroidal and toroidal oscillations, see for example [36]. For definiteness, we focus on torsional oscillations [37–40], a particular class of toroidal oscillations. The torsional oscillations are the only toroidal oscillations in nonrotating stars with a negligible magnetic field [36]. These oscillations can be produced by acting with a torque on a rigid structure, as shown in Fig. 3 for a simple rigid slab. When the applied forces are parallel to the sides of the slab they produce a deformation of the structure. As the external torque vanishes, the slab starts to oscillate around the equilibrium configuration. The restoring force is proportional to the shear modulus and the frequency of the small amplitude oscillations is given by

$$\omega \propto \frac{1}{D}\sqrt{\frac{\nu}{\rho}}\,, \tag{25}$$

where D is the thickness of the slab. The slab can be thought as a local approximation of the CCSC crust, and therefore we expect that the frequency of the crust torsional oscillations has the same qualitative dependence on ν, ρ and the crust thickness, $D = R - R_c$ as in Eq. (25).

Our interest in the torsional oscillations is clearly due to the fact that in the CCSC phase the shear modulus is extremely large and can therefore sustain large amplitude oscillations. We shall show that for a sufficiently thin CCSC crust, the frequency of the oscillations lies in the MHz radio-frequency range, whereas for a thick CCSC crust the frequency of the oscillations lies in the hundreds of Hz range.

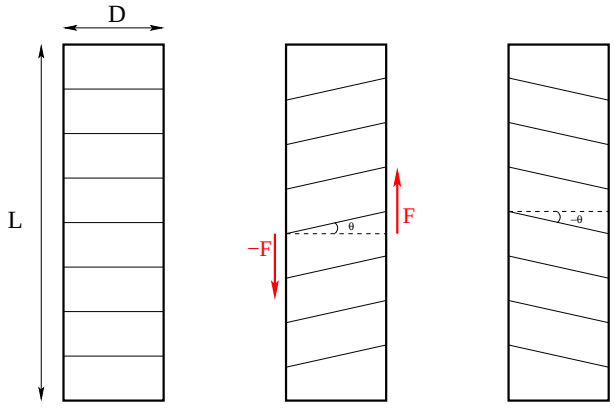

FIG. 3: Pictorial description of the torsional oscillations of a homogeneous two-dimensional slab with $D \ll L$. The equilibrium configuration corresponds to the one in which all the horizontal lines are parallel (left panel). A torque applied at the surfaces of the slab slightly deforms it by an angle θ (central panel). As the applied forces vanish the slab starts to oscillate around the equilibrium configuration, reaching the configuration with deforming angle $-\theta$ (right panel). The restoring force governing the oscillation is proportional to the shear modulus, ν. The applied force determines the amplitude of the oscillation; the frequency of the oscillation is proportional to $\sqrt{\nu/(\rho D^2)}$, where ρ is the matter density of the slab.

Given the spherical symmetry of the nonrotating stars, it is useful to use spherical coordinates for the displace-

ment vector

$$\xi^r_{nl} = 0 \qquad \xi^\theta_{nl} = 0 \qquad \xi^\phi_{nl} = \frac{W_{nl}(r)}{r\sin\theta}\frac{\partial P_l(\cos\theta)}{\partial\theta}e^{i\omega_{nl}t}\,, \tag{26}$$

where l is the angular momentum and n is the principal quantum number indicating the number of nodes. In the following we shall study these oscillations in the Newtonian approximation. We expect that a treatment with full general relativity (GR) should give correction factors of order unity. Given the large uncertainties of the various parameters of the model, it seems appropriate to neglect GR corrections. We shall investigate the GR corrections in a future work.

In the Newtonian limit the velocity perturbation[1] is given by

$$\delta\boldsymbol{u}_{nl} = i\omega_{nl}\boldsymbol{\xi}_{nl}\,, \tag{27}$$

and the amplitude of the horizontal oscillation satisfies the following differential equation

$$\omega^2_{nl}W_{nl} = \frac{\nu}{\rho}\left[-\frac{1}{\nu}\frac{d\nu}{dr}\left(\frac{dW_{nl}}{dr}-\frac{W_{nl}}{r}\right)-\frac{1}{r^2}\frac{d}{dr}\left(r^2\frac{dW_{nl}}{dr}\right) + \frac{l(l+1)}{r^2}W_{nl}\right]. \tag{28}$$

The torsional oscillation extends in the CCSC crust and disappears suddenly in both the CFL phase and the electrosphere. The displacement is discontinuous at these interfaces because both the CFL and the electrosphere have a vanishing shear modulus.

We shall simplify the discussion assuming that the quark matter in the CCSC crust has constant density, $\rho \simeq \rho_R = \rho(R)$. This is a good approximation because in all the considered cases correspond to a CCSC crust a few kilometers thick at most. In any case, the density of quark matter in strange stars does not sharply change, because strange stars are self-bound CSOs. We shall as well neglect the radial dependence of the shear modulus and take it as a constant. In this way the displacement satisfies the following differential equation:

$$\frac{d^2W_{nl}}{dr^2}+\frac{2}{r}\frac{dW_{nl}}{dr}+\left(\frac{\omega^2_{nl}}{v_s^2}-\frac{l(l+1)}{r^2}\right)W_{nl}=0\,, \tag{29}$$

where $v_s = \sqrt{\nu/\rho_R}$ is the shear wave velocity. It is useful to switch to the adimensional variable $y = \omega_{nl}r/v_s$, and to define $W_{nl} = U_{nl}/y$. In this way the above differential equation can be written as

$$U''_{nl}(y)+\left(1-\frac{l(l+1)}{y^2}\right)U_{nl}(y)=0\,. \tag{30}$$

The solution of this equation can be expressed as a sum of spherical Bessel and Neumann functions

$$U_{nl}(y) = c_1 j_l(y) + c_2 n_l(y)\,. \tag{31}$$

After an initial stage in which the crust has been excited by some external agency, we assume that there is no torque acting on both interfaces of the crust. This corresponds to assuming the no-traction condition [36], leading to

$$U'_{nl}(y_1) = 2\frac{U_{nl}(y_1)}{y_1} \qquad U'_{nl}(y_2) = 2\frac{U_{nl}(y_2)}{y_2}\,, \tag{32}$$

where $y_2 = \omega_{nl}R/v_s$ corresponds to the CCSC-electrosphere interface and $y_1 = \omega_{nl}aR/v_s = ay_2$ corresponds to the CFL-CCSC interface. One of the two conditions can be used to eliminate one of the two coefficients in Eq. (31). The other condition determines the quantized frequencies. For definiteness, we shall hereafter assume that the only excited mode is the one with $l = 1$ and with one node[2], $n = 1$. In this case we find that for $a \gtrsim 0.3$ one can use the approximate functions

$$y_2 \simeq \frac{\pi}{1-a} \qquad y_1 \simeq \frac{a\pi}{1-a}\,, \tag{33}$$

and the corresponding oscillation frequency is given by

$$\omega_{11} \simeq 0.06\left(\frac{\nu}{\nu_0}\right)^{1/2}\left(\frac{\delta R}{1\mathrm{km}}\right)^{-1}\left(\frac{\rho_R}{\rho_0}\right)^{-1/2}\mathrm{MHz}\,, \tag{34}$$

where $\delta R = (1-a)R$ and $\rho_0 = 10^{15}\mathrm{g/cm}^3$. Note that for each set of parameters the equation above gives the smaller attainable frequency. Radial overtones, having higher frequencies, could as well be excited by the external agency triggering the oscillation of the crust.

As in the simple example of the slab (see the caption of Fig. 3) the amplitude of the oscillations is determined by the external agency, which fixes the amount of energy of each mode. The frequency of the oscillations is proportional to the shear velocity divided by the crust width.

For definiteness, we shall assume that a fraction α of the energy of a glitch excites the $l = 1, n = 1$ mode; thus

$$\alpha E_{\mathrm{glitch}} = \frac{\rho_R}{2}\int|\delta\boldsymbol{u}_{11}|^2 dV\,, \tag{35}$$

where we shall consider as a reference value $E^{\mathrm{Vela}}_{\mathrm{glitch}} = 3\times10^{-12}M_\odot$ as estimated for the giant Vela glitches. Less energetic glitches, as for the Crab, simply correspond to smaller values of α. Of particular relevance for us is the amplitude of the oscillation at the star surface, because it

[1] Eulerian and Lagrangian perturbations are identical for toroidal oscillations [36].

[2] The mode with $n = 1$ is the first nontrivial mode for $l = 1$. Indeed the mode with no nodes ($n = 0$) corresponds to a global rotation of the star.

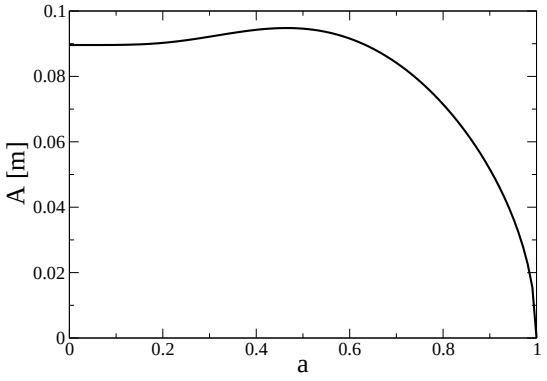

FIG. 4: Function determining the horizontal displacement at the surface of the star associated with the considered torsional oscillation, see Eq. (36).

determines the displacement of the quark electric charge. The displacement does in general depend on the thickness of the crust, on the shear modulus and can be expressed as

$$W_{11}(R) = A(a) \left(\frac{\nu}{\nu_0}\right)^{-1/2} \left(\frac{R}{10\mathrm{km}}\right)^{-1/2} \left(\frac{\alpha E_{\mathrm{glitch}}}{E_{\mathrm{glitch}}^{\mathrm{Vela}}}\right)^{1/2}, \tag{36}$$

where $A(a)$ is reported in Fig.4.

The amplitude of the oscillations is in general quite large, of the order of centimeters, except for $a \simeq 1$. Indeed, the amplitude vanishes for $a = 1$, because this case corresponds to a star completely made of CFL matter. In the following we shall always consider the case in which the crust has a macroscopic extension, much larger than the extension of the positive charge distribution. Notice that considering a perturbation that excites more modes does not qualitatively change the above results. The only effect is a distribution of the total energy among modes with higher frequency.

The fluctuation of the current density induced by periodic horizontal displacement associated with the torsional oscillation is given by $\delta \boldsymbol{J} = e \sum_i Q_i \, n_i(z) \delta \boldsymbol{u}_{11}$. The EM vector field in a point outside the source is given by

$$\delta \mathbf{A}(\mathbf{r}, t) = \int \frac{\delta \mathbf{J}(\mathbf{r}', t_R)}{|\mathbf{r} - \mathbf{r}'|} dV' \,, \tag{37}$$

where $t_R = t - |\boldsymbol{r} - \boldsymbol{r}'|$. We estimate the emitted power by considering the moving electric charges as an oscillating magnetic dipole. In the far field approximation ($|\boldsymbol{r}| \gg |\boldsymbol{r}'|$), and for a coherent emission ($\omega_{11} \ll 1/|\boldsymbol{r}'|$), we obtain that

$$\begin{aligned} P &= \frac{e^2 \pi^4 \omega_{11}^6}{6} \left(\sum_i Q_i \int_0^R dr \, n_i(r) r^3 W_{11}(r) \right)^2 \sin^2(\omega_{11} t) \\ &\simeq \frac{\pi^4 (\omega_{11} R)^6}{6} W_{11}(R)^2 Q_+^2 \sin^2(\omega_{11} t) \,, \end{aligned} \tag{38}$$

where Q_+ is given in Eq. (24). An approximate value of the radiated power is given by

$$P(a) \simeq 6.4 \times 10^{41} \left(\frac{y_2(a)^6 A^2(a)}{y_2(0)^6 A^2(0)}\right) \left(\frac{\nu}{\nu_0}\right)^2 \left(\frac{\rho_R}{\rho_0}\right)^{-3} \left(\frac{R}{10\mathrm{km}}\right)^{-1} \left(\frac{\alpha E_{\mathrm{glitch}}}{E_{\mathrm{glitch}}^{\mathrm{Vela}}}\right) \left(\frac{Q_+}{Q}\right)^2 \mathrm{erg/s} \,, \tag{39}$$

where we have averaged over time and considered as a reference value for the surface charge density $Q = 10^5$ MeV^{3}fm. The values of Q_+ for the two considered models and for two different values of M_s are reported in Table I. The radiated power increases with increasing a, meaning that the thinner the crust, the larger the radiated power (as far as the crust remains larger than the region in which there is a positive electric charge). For example considering $a = 0.9$ we obtain a radiated power of about 10^{45} erg/s. The radiated power increases because the oscillation frequency increases with increasing a. It certainly happens that for $a \to 1$ the amplitude of the oscillation decreases, see Fig. 4, but it does not decrease fast enough to compensate for the increase of the frequency, and thus the product $y_2(a)^6 A^2(a)$ in Eq. (39) increases with increasing a.

Approximate values of the damping time, τ, for the two considered models and for different values of M_s and Δ are reported in Table II, for two values of a. The damping time is computed simply dividing the energy of the oscillation for the corresponding emitted power. This certainly gives a rough, order of magnitude, estimate of the time needed for emitting all the energy. We find that τ decreases with increasing values of M_s and/or Δ. The reason is that with increasing values of M_s the positive charge close to the star surface increases, see Eq. (22) and Table I. With increasing values of Δ the shear modulus increases, see Eq. (3), and therefore the frequency of the oscillations increases. Since $P \propto Q_+^2 \omega_{11}^6$, the dependence on Δ is particularly strong, see Eq. (34) and Eq. (3).

Model	M_s [MeV]	Δ [MeV]	$\tau_{a=0.9}$[s]	$\tau_{a=0.1}$[s]
A	150	5	2.0×10^{-1}	1.7×10^{3}
A	150	25	3.1×10^{-4}	2.8×10^{1}
A	250	5	4.2×10^{-3}	3.7×10^{1}
A	250	25	6.7×10^{-6}	5.9×10^{-2}
B	150	5	3.3×10^{-1}	2.9×10^{3}
B	150	25	5.2×10^{-4}	4.6×10^{0}
B	250	5	8.2×10^{-3}	7.3×10^{1}
B	250	25	1.3×10^{-5}	1.2×10^{-2}

TABLE II: Approximate values of the damping times for the two considered models for two different values of the strange quark mass and of the gap parameter. In the third column we have assumed that $a = 0.9$, meaning that the CCSC crust is about 0.7 km (1.1 km) thick for Model A (Model B). In the fourth column we have taken $a = 0.1$, meaning that the CCSC crust is about 6.4 km (9.8 km) thick for Model A (Model B).

So far we have assumed that the electrosphere does not screen the radiated photons. However, it is conceivable that a sizable fraction of the emitted energy will be scattered by the electrosphere. The detailed modelization of the electrosphere and of the interaction with the photons emitted by the positive charged quark layer is a nontrivial problem, see for example [22, 41–43]. We shall estimate the absorbed fraction considering a completely degenerate electron gas at small temperature [41]. The absorption is due to the Thomson scattering of photons off degenerate electrons and leads to an exponential reduction of the emitted power. Assuming that electrons are degenerate and considering that temperature corrections, of order T/m_e, can be neglected, one finds that the intensity of the emitted radiation is suppressed by [41]

$$\eta = \exp\left(-\frac{1.129}{6\pi^2}\sqrt{\frac{3\pi}{2\alpha_{\rm em}}}\sigma_T V_0^2\right) , \qquad (40)$$

where $\sigma_T = 8\pi/3(\alpha_{\rm em}^2/m_e^2)$ is the total Thomson cross section. For the considered values of the surface potential, see Table I, we obtain suppression factors of order 0.1.

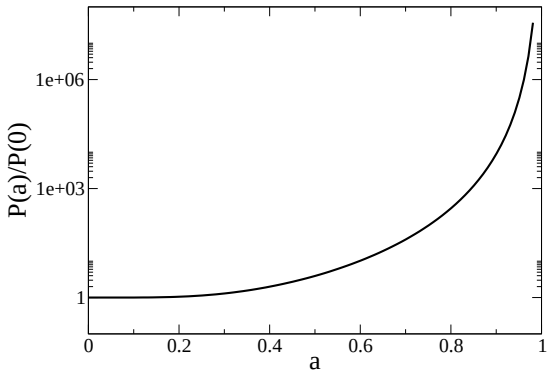

FIG. 5: Radiated power, see Eq. (39), as a function of the ratio between the core radius and the star radius, a. The radiated power is normalized to the value for $a = 0$, corresponding to a strange star with a rigid crust extending from the surface down to the center of the star.

V. CONCLUSIONS

We have discussed two very simple strange star models entirely composed of deconfined color superconducting matter. Our star models are very similar to those proposed in [22] for the discussion of $r-$mode oscillations. We assume that the star core is composed by CFL matter and there is a crust of rigid CCSC quark matter. The size of the star crust is unknown, because it depends on the detailed values of the strange quark mass and of the gap parameters, which are very uncertain. For this reason we have treated the ratio between the core radius and the star radius as a free parameter.

In our treatment of the crust we have determined the equilibrium charge configuration, in Sec. III, using the free Fermi gas distributions but at the same time we have considered CCSC matter, in Sec. IV, as a rigid crystalline structure. These two facts may seem to be in contradiction. However, in the relevant crystalline phases, quarks close to the Fermi sphere have a linear dispersion law [15, 44], which indeed mimics the behavior of free quarks. The effect of the condensate is to induce a direction dependent Fermi velocity. Moreover, not all quarks on the top of the Fermi sphere are paired. For these reasons we have assumed that the EM properties of the CCSC phase are similar to those of unpaired quark matter. What is rigid is the modulation of the underlying quark condensate that can be seen as the structure on the top of which quarks propagate. This treatment of the EM properties of the CCSC phase is in our opinion an educated assumption. A detailed study of the EM properties of the CCSC phase is necessary to substantiate this approach.

The discussion of the quark matter surface can certainly be improved including condensation effects, following for example the discussion in [45], or viscous damping below the star crust as in [46]. Moreover it would be interesting to study whether strangelet crystals could form on the star surface [47]. One should investigate whether these strangelet nuggets might coexist with the CCSC phase, presumably assuming that the surface tension of quark matter is not too large, eventually leading to a drastic reduction of the surface charge density.

In our simple treatment, we estimate the emitted energy of the torsional oscillations using an oscillating magnetic dipole. The emitted power is extremely large, for stars with a small CFL core it is of the order of $10^{41}\eta$

erg/s, where η is a screening factor due to the presence of the electrosphere, estimated in Eq. (40). The emitted power steeply increases with increasing values of a, see Fig. 5, meaning that stars with a large CFL core and a thin CCSC crust would probably emit all the oscillation energy in milliseconds. For a sufficiently thin crust, say hundreds of meters thick, we expect that the emission is at the MHz frequency.

Given the large emitted power, it is tempting to compare our results with the most powerful observed EM emissions. The radio bursts observed from Rotating Radio Transients have a duration of few milliseconds and the associated flux energy is extremely large [48]. However, the observed frequencies are of the order of GHz, see [49–51], whereas we found that the frequencies associated with the $n = 1, l = 1$ mode of a star with a 1 km CCSC crust are of the order of tens of kHz. If the crust is thinner, say a few centimeters thick, then GHz frequencies can be attained, but in this case the emitted power, estimated by Eq. (39), is extremely large and the damping time should be much less than the observed milliseconds. A loophole might be that by Eq. (39) we are overestimating the emitted power by orders of magnitude. The reason is that in Eq. (39) we are using the coherent emission approximation, which conceivably breaks down at such large frequencies. Moreover, we are assuming the presence of a net positive charge, with electrons only providing a screen for the emitted power. A more refined treatment should include the effect of the star magnetic field which might strongly couple the oscillation of the star and of the electrosphere. Therefore, future work in this direction is needed to clarify how the presented discussion of the emitted EM power changes in the presence of strong magnetic fields, see for example [52, 53]. A different possibility is that there exists a mechanism for exciting predominantly modes with higher angular momentum and/or higher principal quantum numbers. In this case, frequencies larger than tens of kHz could be reached for stars with a thick crust, as well.

Different powerful phenomena of great interest are giant magnetar x-rays flares [54]. The observation of these flares has posed a challenge to strange stars with no crust [55]. The standard explanation of these flares is indeed related with the seismic vibrations of the crust triggered by a starquake. Typical frequencies are of the order of hundreds of Hz at most and the emitted luminosities is of the order of $10^{44}-10^{46}$ erg/s. The measured decaying time is of order of minutes. In our model, oscillations of hundreds of Hz can be reached only if the shear modulus is sufficiently small, of the order of $\nu_0 10^{-4}$, making it comparable with standard nuclear crusts, and if the CCSC crust is sufficiently thick, say of the order of a few kilometers, meaning that $a \sim 0.1$. For these small values of a the damping time can be of the order of hundreds of seconds, see the last column in Table II. Basically, our bare strange star model has frequency and decay times compatible with magnetar flares only if it has the same structure of a standard neutron star. The caveat is that these flares are observed in magnetars, which are CSOs expected to have a large magnetic field. In our simple treatment we have neglected the effect of the background magnetic field, which however in the case of magnetars could be sizable.

We have neglected the effect of the temperature, as well. Although temperature effects are negligible for strange stars older than ~ 10 s [56], when the temperature has dropped below the MeV scale, it would be interesting to see what is the effect of a large, say ~ 10 MeV temperature, see for example the discussion in [41, 57]. Unfortunately, the shear modulus has only been computed at vanishing temperature [26]. A detailed study of the temperature dependence of the shear modulus and of the response of the CCSC structure to the temperature is needed to ascertain the correct temperature dependence of the torsional oscillations. However, let us assume that the CCSC structure has already formed when the temperature is of the order of few MeV, and that it responds to the temperature as a standard material, meaning that with increasing temperature the shear modulus decreases. From Eq. (34) it follows that the frequency of the torsional oscillation decreases, and, from Eq. (36), that the amplitude increases. Moreover, an increasing temperature should lead to an increase of the number densities of the light quarks and electrons, leading to a larger Q_+. The overall effect on the radiated power is not obvious, because in Eq. (38) we have that ω_{11} decreases, but W_{11} and Q_+ increase; therefore a careful study of the various contributions is necessary. Regarding the emission mechanisms of the electrosphere, one should consider the various processes that become relevant at nonvanishing temperature. In particular, e^+e^- production is believed to be the dominant process at high temperature [58–61].

Finally, note that in the evaluation of the horizontal displacement one should include the radial dependence of the shear modulus and of the matter densities as well as GR corrections, which are expected to be small, but should nevertheless be considered for a more refined study.

Acknowledgments

We thank M. Alford and I. Bombaci for insightful discussions.

[1] F. Weber, editor, *Pulsars as astrophysical laboratories for nuclear and particle physics*, 1999.

[2] D. D. Ivanenko and D. F. Kurdgelaidze, Astrophysics **1**,

251 (1965).
[3] D. Ivanenko and D. Kurdgelaidze, Lett.Nuovo Cim. **IIS1**, 13 (1969).
[4] J. C. Collins and M. J. Perry, Phys. Rev. Lett. **34**, 1353 (1975).
[5] G. Baym and S. Chin, Phys.Lett. **B62**, 241 (1976).
[6] E. Witten, Phys.Rev. **D30**, 272 (1984).
[7] C. Alcock, E. Farhi and A. Olinto, Astrophys.J. **310**, 261 (1986).
[8] P. Haensel, J. Zdunik and R. Schaeffer, Astron.Astrophys. **160**, 121 (1986).
[9] J. Madsen, Lect.Notes Phys. **516**, 162 (1999), [astro-ph/9809032].
[10] I. Barbour *et al.*, Nucl.Phys. **B275**, 296 (1986).
[11] G. Aarts, 1312.0968.
[12] A. Yamamoto, Phys.Rev.Lett. **112**, 162002 (2014), [1402.3049].
[13] K. Rajagopal and F. Wilczek, hep-ph/0011333.
[14] M. G. Alford, A. Schmitt, K. Rajagopal and T. Schafer, Rev.Mod.Phys. **80**, 1455 (2008), [0709.4635].
[15] R. Anglani *et al.*, Rev. Mod. Phys. **86**, 509 (2014).
[16] M. G. Alford, K. Rajagopal and F. Wilczek, Nucl.Phys. **B537**, 443 (1999), [hep-ph/9804403].
[17] M. G. Alford and K. Rajagopal, JHEP **0206**, 031 (2002), [hep-ph/0204001].
[18] M. G. Alford, C. Kouvaris and K. Rajagopal, Phys.Rev.Lett. **92**, 222001 (2004), [hep-ph/0311286].
[19] M. G. Alford, J. A. Bowers and K. Rajagopal, Phys.Rev. **D63**, 074016 (2001), [hep-ph/0008208].
[20] K. Rajagopal and R. Sharma, Phys.Rev. **D74**, 094019 (2006), [hep-ph/0605316].
[21] M. Mannarelli, 1401.7551.
[22] G. Rupak and P. Jaikumar, Phys. Rev. C **88**, 065801 (2013).
[23] R. Casalbuoni, R. Gatto, M. Mannarelli and G. Nardulli, Phys.Lett. **B511**, 218 (2001), [hep-ph/0101326].
[24] R. Casalbuoni, R. Gatto, M. Mannarelli and G. Nardulli, Phys.Rev. **D66**, 014006 (2002), [hep-ph/0201059].
[25] R. Casalbuoni, E. Fabiano, R. Gatto, M. Mannarelli and G. Nardulli, Phys.Rev. **D66**, 094006 (2002), [hep-ph/0208121].
[26] M. Mannarelli, K. Rajagopal and R. Sharma, Phys.Rev. **D76**, 074026 (2007), [hep-ph/0702021].
[27] T. Strohmayer, H. M. van Horn, S. Ogata, H. Iyetomi and S. Ichimaru, Astrophys. J. **375**, 679 (1991).
[28] L.-M. Lin, Phys.Rev. **D76**, 081502 (2007), [0708.2965].
[29] B. Haskell, N. Andersson, D. Jones and L. Samuelsson, 0708.2984.
[30] L.-M. Lin, Phys.Rev. **D88**, 124002 (2013), [1311.2654].
[31] B. Knippel and A. Sedrakian, Phys.Rev. **D79**, 083007 (2009), [0901.4637].
[32] N. Andersson, D. Jones and K. Kokkotas, Mon.Not.Roy.Astron.Soc. **337**, 1224 (2002), [astro-ph/0111582].
[33] M. G. Alford, M. Braby, M. W. Paris and S. Reddy, Astrophys.J. **629**, 969 (2005), [nucl-th/0411016].
[34] R. P. Negreiros, F. Weber, M. Malheiro and V. Usov, Phys.Rev. **D80**, 083006 (2009), [0907.5537].
[35] M. G. Alford, S. Han and S. Reddy, J.Phys. **G39**, 065201 (2012), [1111.3937].
[36] P. N. McDermott, H. M. van Horn and C. J. Hansen, Astrophys. J. **325**, 725 (1988).
[37] M. A. Ruderman, Nature (London) **218**, 1128 (1968).
[38] M. Ruderman, Nature (London) **225**, 619 (1970).
[39] C. J. Hansen and D. F. Cioffi, Astrophys. J. **238**, 740 (1980).
[40] B. L. Schumaker and K. S. Thorne, Mon.Not.Roy.Astron.Soc.**203**, 457 (1983).
[41] K. Cheng and T. Harko, Astrophys.J. **596**, 451 (2003), [astro-ph/0306482].
[42] R. Picanco Negreiros, I. N. Mishustin, S. Schramm and F. Weber, Phys.Rev. **D82**, 103010 (2010), [1008.0277].
[43] B. Zakharov, Phys.Lett. **B690**, 250 (2010), [1003.5779].
[44] R. Casalbuoni *et al.*, Phys.Lett. **B575**, 181 (2003), [hep-ph/0307335].
[45] M. G. Alford, K. Rajagopal, S. Reddy and F. Wilczek, Phys.Rev. **D64**, 074017 (2001), [hep-ph/0105009].
[46] L. Lindblom, B. J. Owen and G. Ushomirsky, Phys.Rev. **D62**, 084030 (2000), [astro-ph/0006242].
[47] P. Jaikumar, S. Reddy and A. W. Steiner, Phys.Rev.Lett. **96**, 041101 (2006), [nucl-th/0507055].
[48] M. A. McLaughlin *et al.*, Nature (London) **439**, 817 (2006), [astro-ph/0511587].
[49] D. Lorimer, M. Bailes, M. McLaughlin, D. Narkevic and F. Crawford, 0709.4301.
[50] D. Thornton *et al.*, Science **341**, 53 (2013), [1307.1628].
[51] J. M. Cordes, Science **341**, 40 (2013).
[52] K. Glampedakis, L. Samuelsson and N. Andersson, Mon.Not.Roy.Astron.Soc.Lett. **371**, L74 (2006), [astro-ph/0605461].
[53] Y. Levin, Mon.Not.Roy.Astron.Soc. **377**, 159 (2007), [astro-ph/0612725].
[54] T. E. Strohmayer and A. L. Watts, Astrophys.J. **632**, L111 (2005), [astro-ph/0508206].
[55] A. L. Watts and S. Reddy, Mon.Not.Roy.Astron.Soc. **379**, L63 (2007), [astro-ph/0609364].
[56] D. Page and V. V. Usov, Phys.Rev.Lett. **89**, 131101 (2002), [astro-ph/0204275].
[57] V. Usov, T. Harko and K. Cheng, Astrophys.J. **620**, 915 (2005), [astro-ph/0410682].
[58] V. Usov, Phys.Rev.Lett. **80**, 230 (1998), [astro-ph/9712304].
[59] V. V. Usov, Astrophys.J. **550**, L179 (2001), [astro-ph/0103361].
[60] A. Aksenov, M. Milgrom and V. V. Usov, Mon.Not.Roy.Astron.Soc. **343**, L69 (2003), [astro-ph/0306361].
[61] A. Aksenov, M. Milgrom and V. V. Usov, Astrophys.J. **609**, 363 (2004), [astro-ph/0309014].